

Tuning morphology and magnetism in epitaxial $L1_0$ -FePt films

P. Lupo^{1,a}, J. Orna², F. Casoli¹, L. Nasi¹, P. Ranzieri¹, D. Calestani¹, P. Algarabel³, L. Morellón⁴, F. Albertini¹

¹ IMEM-CNR, Parco Area delle Scienze 37/a, Parma, 43124 (Italy)

² Centro Nacional de Energías Renovables (CENER), Ciudad de la Innovación 7, 31621-Sarriguren (Spain)

³ Instituto de Ciencia de Materiales de Aragón, Universidad de Zaragoza-CSIC, Facultad de Ciencias, Zaragoza (Spain)

⁴ Instituto de Nanociencia de Aragón, Universidad de Zaragoza, Zaragoza (Spain)

Abstract. In this work, well-ordered epitaxial FePt thin films have been grown by RF sputtering on two different substrates (MgO (100) and SrTiO₃ (100)) and the effect of different lattice parameters between the substrate and FePt film on morphology and magnetic behavior has been considered. Growth conditions have been optimized to obtain different morphologies and magnetic behaviors.

1 Introduction

In the last decade, many studies have been conducted to investigate the growth of $L1_0$ -ordered FePt films, characterized by a high magneto-crystalline energy density (K_a) and c-axis orientation perpendicular to the film plane. These works focused on technical applications as well as the basic mechanism of $L1_0$ ordering, magnetic properties and morphology tuning. To induce the required (001) texture, deposition on single crystalline MgO (100) is usually carried out [1, 2]. The deposition on SrTiO₃ (STO) (100), with reduced misfit value ($\delta=1.5\%$ with a $STO=0.393$ nm) between the two materials, makes this substrate an attractive choice. This may increase the possibility of tuning morphology and magnetism of $L1_0$ -FePt thin films, fitting many technological purposes (i.e., perpendicular magnetic recording media, spintronics devices) [3,4]. In this work the correlation among FePt thin film morphology, crystal structure and magnetism has been investigated by comparing the results obtained on the two substrates (i.e., MgO and STO) at the same growth conditions. Moreover, the effect of lattice misfit on structure, morphology and magnetic properties has been studied. Higher structural quality, order parameter and K_a have been obtained on FePt film grown on SrTiO₃ substrate, at low growth temperature, compared with previous works [5,6]. Promising results on grains separation and high structural order have been obtained on STO without the employment of any other solution (i.e., seed layer, buffer layer, thermal treatments) and obtaining an ordering temperature of the FePt alloy lower than on MgO.

2 Experimental

FePt thin films with thickness of 15 nm have been grown on MgO (100) and SrTiO₃ (100) substrates by a RF sputtering with base pressure lower than 3×10^{-8} mbar. Fe and Pt elemental layers have been alternately deposited on the heated substrate, with a nominal atomic composition of

^a e-mail: lupo@imem.cnr.it

$Fe_{57}Pt_{43}$. During the deposition an Ar pressure of 1.5×10^{-2} mbar and growth temperature (T_G) of 450° C have been kept constant. T_G has been measured by a thermocouple directly in contact with the substrate. Structural characterization has been performed by means of X-ray diffraction (XRD) in $\theta - 2\theta$ configuration, using a Bruker AXS D8 diffractometer. Sample surface morphology has been investigated by a Dimension 3100 Atomic Force Microscope (AFM) equipped with a Nanoscope IVa controller (Veeco Instruments). Moreover, samples have been measured in cross section by high-resolution transmission electron microscopy (HRTEM) and high angle annular dark field (HAADF) in scanning mode (STEM) with a Jeol 2200FS microscope working at 200 keV. Hysteresis loops have been investigated at room temperature by alternating gradient force (AGFM) and SQUID magnetometers. Magnetization curves have been measured up to 2 T by AGFM in both parallel and perpendicular directions with respect to the film plane, and up to 5.5 T by SQUID magnetometer.

3 Results

HRTEM and selected area electron diffraction (SAD) investigations show the epitaxial growth of FePt, on both MgO and SrTiO₃ substrates, with the orientation relationship $FePt(001) < 100 > || MgO(STO)(100) < 100 >$. The presence of the $L1_0$ ordered phase has been revealed by the appearance of the (001) superlattice spots in the SAD patterns and confirmed by HRTEM, which show alternating Pt and Fe monoatomic layers along the film thickness.

The XRD spectra in figure 1(a) and 1(b) show only the 00l reflections of the ordered $L1_0$ -phase, consistently with the TEM analysis. The appearance of $L1_0$ FePt (003) and (004) peaks (not show here) confirms the texture and the high order degree on STO substrate. Following Cebollada *et al.* [7] the order parameter (S) for FePt film is: 0.58 on MgO and 0.85 on STO, at 450° C. Moreover, *Laue* oscillations are found for (001) and (002) peaks on film grown on STO substrate, which is a remarkable sign of the high structural order.

Figure 2(a) shows AFM images taken on films grown on

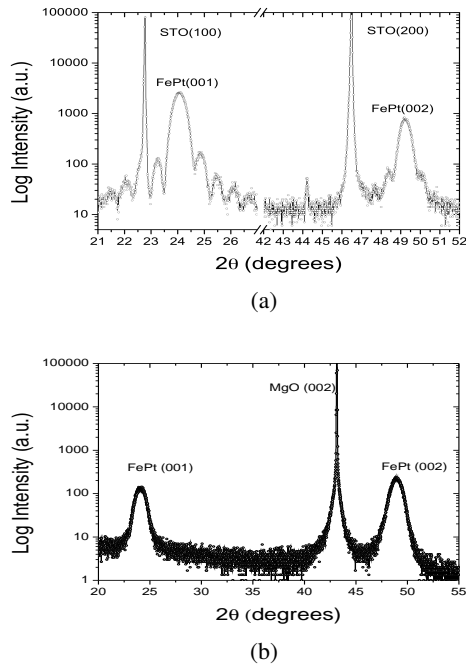


Fig. 1. XRD patterns of FePt thin film grown on STO (a) and MgO (b) substrates at 450°C.

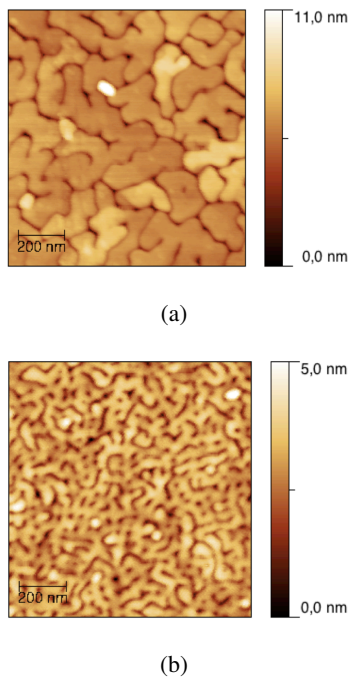


Fig. 2. AFM images of FePt thin film grown on STO (a) and on MgO (b) substrates at 450°C.

STO at 450°C. Morphology exhibits a island-like pattern and, consequently, RMS roughness is substantially high (0.92 nm). In order to examine grains separation, cross section TEM analysis has been performed (Fig.3(a)), showing a well separated grain structure with gaps between neighbor grains of about 3-4 nm and maximum grains height of 16 nm. The TEM cross section analysis shows regular shaped grains with atomically flat top surface and visible

faceting.

On MgO substrates, FePt morphology is characterized by semicontinuous maze-like pattern, as shown in figure 2(b), with a RMS roughness of 0.55 nm. In particular, coalescence at the grains base and irregular grains shape are observable and these features are confirmed by HAADF-TEM (Fig.3(b)).

The hysteresis loops of the FePt films grown on MgO

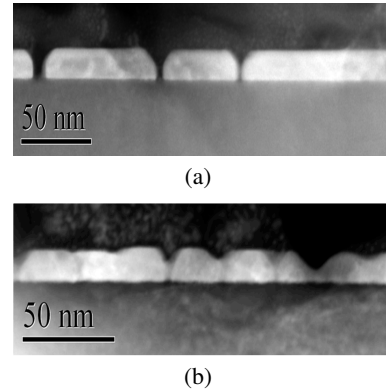


Fig. 3. HAADF STEM image of 15nm FePt film grown at 450°C on STO (a) and MgO (b).

(Fig.4(a)) and on STO (Fig.4(b)) show easy magnetization c-axis oriented perpendicular to the film plane. In the latter, an artifact of the SQUID measurement is present close to the zero applied field, which is due to change in sensitivity scale and/or sample contaminations [8]. Relevant magnetic properties of thin films are reported in table 1. The uniaxial anisotropy energy density (K_a) and the anisotropy field (H_a) have been roughly evaluated by extrapolating the hard-axis hysteresis loop (in-plane magnetization) to magnetization saturation value obtained from easy-axis hysteresis loop. Values of saturation magnetization (M_s) and remanence ratio (M_r/M_s) have been obtained for film grown on MgO (750 ± 30 emu/cm³; 0.014), and also for films grown on (870 ± 38 emu/cm³; 0.011). Moreover, coercive field (H_c) and anisotropy field (H_a),

Table 1. Coercivity (H_c), anisotropy field (H_a), remanence ratio (M_r/M_s) and saturation magnetization (M_s) at 450°C on the two substrates

Substrate	H_c (T)	H_a (T)	M_r/M_s	M_s (emu)
MgO	0.4	4.3 ± 0.3	0.014	750 ± 30
STO	0.75	7.5 ± 0.5	0.011	870 ± 38

have been obtained by extrapolating the parallel magnetization curves to saturation. H_a measured for FePt as-grown on STO substrate, shows higher values respect to film grown on MgO

4 Discussion

The lower misfit on STO substrates (i.e., $\Delta=1.28\%$) allows a better FePt order degree compared with growth on MgO

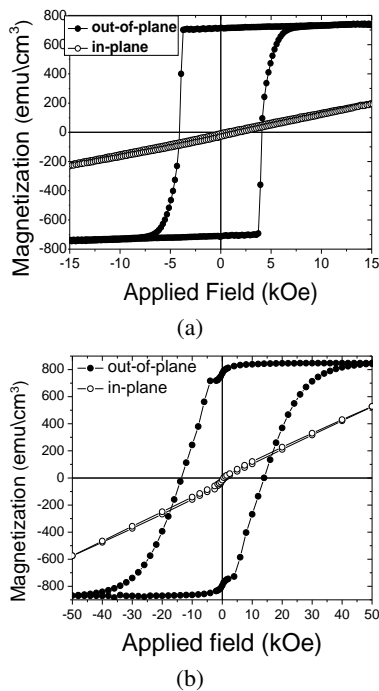


Fig. 4. Hysteresis loops measured on FePt grown on (a) MgO and (b) SrTiO₃ at 450°C. Magnetic field is applied perpendicular to film plane (full symbols) and parallel (open symbols) to plane.

(i.e., $\Delta=8.55\%$) at $T_G=450^\circ\text{C}$. $L1_0$ -ordered phase has been obtained at lower temperatures than in [1] and [5], this is partially due to the alternate sputtering deposition method, which is very effective in fabricating the FePt ordered alloy at low temperatures [9]. Evidence of epitaxy and $L1_0$ order have been deduced by the structural analysis. The epitaxial relationship $FePt(001) < 100 > || MgO(STO)(100) < 100 >$ on both substrates. Better structural coherence of FePt film on STO, than on MgO substrate, is demonstrated by *Laue* oscillations for (001) and (002) peaks only spotted on STO substrate. Higher order parameter values have been reported in previous works [10] on FePt with a thickness of 10 nm, this difference could be ascribed to a dependence on film thickness of the ordering processes [11]. Morphology is shown to be sensitive to the misfit between the film and the substrate. As found in the literature (e.g., [12], [13]), FePt films grow as islands on top of the substrate in the Volmer-Weber three-dimensional (3D) growth mode in early stage, then small islands coalesce into larger islands, which exhibit the equilibrium shapes [14]. These phenomena are at the origin of the interconnected maze-like structures found in the FePt on MgO (Fig.2(b)). In the case of film grown on STO substrate, the better crystal structural quality allows the formation of larger and isolated islands with low strain and with the same orientation as $L1_0$ FePt equilibrium shape [15], since not constrained by the substrate.

The hysteresis loops, shown in figures 4(a) and 4(b), testify the large amount of ordered $L1_0$ phase with easy magnetization axis oriented perpendicular to the film plane and low parallel remanence. In the case of MgO substrate, the strong magnetic interaction between neighboring grains is responsible for the higher loop steepness and sharper magnetisation reversal. On STO, despite the higher structural

quality of the films, the magnetic disorder caused by grain size inhomogeneity and reduced interaction between separated grains determine a smoother slope in the hysteresis loop [16]. In this case, it is also worth mentioning that the maximum applied field (5.5 T) is possibly too low for completely saturating the sample. The difference in lattice parameter between FePt and the substrate is one of the key factors to obtain high magnetocrystalline anisotropy with easy axis perpendicular to the substrate. On MgO substrates, due to higher misfit compared to STO, perpendicular magnetic anisotropy at 450°C is $2.1 \pm 0.2 \times 10^6 \text{ J/m}^3$. On the other hand, film grown on STO substrate shows a magneto-crystalline anisotropy constant of $3.2 \pm 0.3 \times 10^6 \text{ J/m}^3$, although lower misfit. This improvement in the magnetic anisotropy may be related to the interplay of different forces that promote an increasing of ordered phase obtained by the growth on STO. These forces combined with the higher order degree and a better structural quality on STO allow higher K_a on STO than on MgO. Moreover, for the growth on STO substrate, a larger exposed grains surface and a lower misfit dislocations result in a higher magnetic saturation. Hence, regarding perpendicular coercivity, the film morphology on STO causes an increasing in H_c up to the value of 0.75 T. On the other hand, more regular film morphology on MgO is responsible for the moderate values of coercivity compared to the results of Takahashi *et al.* [1] and Shima *et al.* [12]. Finally, H_a changes are linked to the FePt $L1_0$ -ordered fraction, as shown in [17].

5 Conclusion

Epitaxially FePt films with a thickness of 15 nm have been grown on MgO(100) and SrTiO₃(100) at 450°C. The highest fraction of $L1_0$ phase with a complete epitaxy has been obtained on STO substrate. Recent studies on the same substrate show a ordering temperature less than 450°C. Moreover, studies on thinner films suggest a dependence on the thickness of ordering temperature. Grains separation has been found on film grown on STO together with an evident grain faceting along specific crystallographic directions. These grain boundaries could act as pinning sites for the magnetic domain wall increasing coercivity and together with an higher degree of order and magneto-crystalline anisotropy value increase H_c value compared with film grown on MgO. On STO the lowest misfit enhances transition to order- $L1_0$ phase easier and at lower order temperature than on MgO, without the employ of dynamic stress (e.g.,[18]) or buffer layers (e.g.,[19]). The hysteresis loop shape points out a homogenous distribution of grains dimension on MgO substrate, which is related to sharp reversal field, instead on STO the wide distribution of islands size avoid a sharp reversal process.

The better growth of FePt film on SrTiO₃ than MgO substrate concerns not only morphology, i.e. grain separation and faceting, but also structural, i.e. higher S value, and magnetic, i.e. higher H_a and lower M_r . This is a noticeable result for magnetic recording technology, where the research for high-anisotropy materials supporting thermal stability is become an important issue. This may also open a wide scenario of applicability in other magnetic heterostructures as: spin valves or perpendicular magnetic tunnel junctions and spin torque switching devices.

References

1. Takahashi, Y.K., Hono K. Shima T., Takanashi K., Journ. Magn. Magn. Mat. **267**, (2003) 248
2. Kim M., Shin S., Kang, K., Appl. Phys. Lett. **80**, (2002) 3802
3. Yoshikawa M., Kitagawa E., Nagase T., Daibou T., Ieee T. Magn **44**, (2008) 2573
4. Piramanayagam S.N., Srinivasan K., Journ. Magn. Magn. Mat. **321**, (2009) 485
5. Zha C., He S., Ma B., Zhang Z., F.X.Gan, Q.Y.Jin, Ieee T. Magn **44**, (2008) 3539
6. Ding Y.F., Chen J.S., Liu E., J. Cryst. Growth. **276**, (2005) 111
7. Ce Bollada A., Farrow R.F.C., Toney, M. F., *Structure and magnetic properties of chemically ordered magnetic binary alloys in thin film form.*
In: Nalwa HS, editor. *Magnetic Nanostructures* (Los Angeles: American Scientific Publisher; 2002. p. 93.)
8. Ney A., J. Magn. Magn. Mat. **320**, (2008) 3341.
9. Shima T., Moriguchi T., Mitani S., Takanashi K., Appl. Phys. Lett. **80**, (2002) 288
10. Casoli F., Albertini F., Nasi L., Fabbri S., Bocchi C., Germini F., Luches P., Rota A., Valeri S., J. Appl. Phys. **103**, (2008) 043912
11. Toney M.F., Lee W.-Y., Hedstrom J.A., Kellock A., J. Appl. Phys. **93**, (2003) 9902
12. Shima T., Takanashi K., Takahashi Y., Hono K., Appl. Phys. Lett. **81**, (2002) 1050
13. Peng Y., Zhu G., Laughlin D., J. Appl. Phys. **99**, (2006) 08F907
14. R. Koch, J. Phys.: Condens. Matter **6**, (1994) 9519
15. Hong S., Yoo M.H., J. Appl. Phys. **97**, (2005) 084315
16. Jagla E. A., Phys. Rev. B **72**, (2005) 094406.
17. Ristau R.A., Barmak K., Lewis L.H., J. Appl. Phys. **86**, (1999) 4527
18. Li X., Liu B., Li F., Sun H., Li W., Yang C., Zhang X., Scripta Materialia **57**, (2007) 77
19. Seki T., Shima T., Takanashi K., Takahashi Y., Mat-subara E., Takahashi Y., Hono K., J. Appl. Phys. **96**, (2004) 1127